Radio Monitoring Coverage Assessment Based on Nighttime Light Remote Sensing Data

Song Yan Mo, Chong Xing Huang, Jing Jing Yang, and Ming Huang

Abstract – Improving coverage has been one of the main objectives of radio monitoring network construction, and radio monitoring coverage assessment has become a matter of concern. This article uses a graph model to associate nighttime light remote sensing (NTL-RS) data of a particular area with the corresponding spatial field strength (SFS) data obtained from an elastic wave propagation simulation. The geographic coverage and population coverage of the radio monitoring station are characterized through adjacency matrix calculation. Taking Wuhua District, Kunming, Yunnan Province, as an example, two radio services are available. Results showed that the geographic coverage of digital TV and FM radio was 21.06% and 27.96%, respectively, while the respective population coverage was 48.1% and 57.5%. When considering the light intensity weight, the weighted population coverage was 92.9% and 94.3%. The method proposed in this article is vital for the scientific assessment of radio monitoring coverage.

1. Introduction

Coverage prediction is essential for wireless network planning by operators and a basic requirement for offering users high-quality services [1]. It is also crucial in the construction of radio monitoring networks. One of China's main objectives in building its radio monitoring network since the "12th Five-Year Plan" has been to improve radio monitoring coverage, and this trend persisted to the "14th Five-Year Plan" [2]. According to the requirements of the Ministry of Industry and Information Technology [3], China has conducted radio monitoring coverage assessment from various dimensions, including spatial coverage, geographic coverage, site coverage, and time and frequency domain coverage capabilities. Numerous industry experts and scholars have conducted computational simulations based on this specification. For instance, [4] proposed a geographic coverage assessment scheme for VHF and UHF fixed monitoring stations by calculating the geographic coverage of several specific radio services provided by fixed monitoring stations. Others proposed a geographic coverage evaluation method for fixed monitoring stations in land border areas for the topography of border areas and the characteristics of frontier radio work [5]. Researchers compared and analyzed the differences in the geographic coverage of radio monitoring (GCRM) in Yunnan and Henan Provinces and found that the topography is a key factor in determining the geographic coverage of the two provinces [6]. In [7], an evaluation scheme was proposed for the coverage area of VHF and UHF fixed monitoring stations. However, the relentless pursuit of high geographic coverage can result in a waste of radio monitoring resources. Radio monitoring should first consider covering the population aggregation area, i.e., the primary goal should be to improve population coverage of radio monitoring (PCRM). Because nighttime light remote sensing (NTL-RS) data are important data that reflect the degree of population aggregation and intensity of human activities [8–11], this article combines NTL-RS data with spatial field strength (SFS) data simulated by ICS telecom (EV 15.6.2) and proposes a monitoring coverage assessment method based on a graph model, which has practical significance for planning and designing radio monitoring networks. To the best of our knowledge, the existing methods mainly focus on geographic coverage [12, 13], and there is no report on the population coverage of radio services.

The rest of this article is organized as follows. We describe the SFS data set generated by simulation in the Section 2. Section 3 introduces the NTL-RS data set and its preprocessing. The radio monitoring coverage graph model proposed to correlate the SFS data set and the NTL-RS data set is illustrated in Section 4. The calculation of geographic coverage and population coverage is illustrated in Section 5. Results and a discussion are given in Section 6. Finally, conclusions are drawn in Section 7.

2. Spatial Field Strength Data Set

The SFS data sets for FM radio (100 MHz) and digital TV (700 MHz) were obtained using electromagnetic wave propagation simulations in ICS Telecom software [14]. Simulation parameters are shown in Tables 1 and 2, with case A representing the national standard simulation condition [3]. The simulation radius is set to 50 km. The station site is the Huizhou building of Yunnan University, and the propagation model is ITU-R P.1546. Figure 1 shows the FM radio coverage maps obtained under different

Manuscript received 10 December 2022. This work was supported by the National Natural Science Foundation of China. (61963037, 62261059, and 61863035)..

Song Yan Mo, Jing Jing Yang, and Ming Huang are with the School of Information Science and Engineering, Yunnan University, No.2 North Cuihu Road, Kunming, 650091, China; e-mail: 1531588654@qq.com, yangjingjing@ynu.edu.cn, huangming@ynu.edu.cn.

Chong Xing Huang is with Faculty of Social and Historical Sciences, University College London, Gower Street, London, WC1E 6BT, United Kingdom; e-mail: chongxing.huang.21@ucl.ac.uk.

Table 1. Simulation parameters of SFS data of FM radio

FM radio	Geographic coordinates	Transmitting power (dBW)	Antenna height (m)	Feeder loss (dB)
Case A	25.054076, 102.703556	50	70	0
Case B	25.054076, 102.703556	40	70	0
Case C	25.054076, 102.703556	50	35	0
Case D	25.054076, 102.703556	50	70	5

conditions, and the digital TV coverage map is displayed in Figure 2.

3. NTL-RS Data Set

NTL-RS data originated from the Defense Meteorological Satellite Program (DMSP) 30 years ago. The spatial resolution was initially 2700 m [15], which was increased to 740 m 10 years later with the launch of the Suomi National Polar-Orbiting Partnership (NPP) [16]. In recent years, China has made a breakthrough in remote sensing technology, and the spatial resolution of the Luojia-101 developed by Wuhan University reached 130 m. Recently, researchers in [17] used a crewless aircraft as the remote sensing platform and a portable camera device as the sensor to obtain a set of voluntary passenger aircraft night remote sensing (VPAN-RS) images with a spatial resolution of less than 15 m. As a result of the NTL-RS data's increasing spatial resolution, studies in various monitoring fields have moved to smaller scales with improved accuracy. Table 3 shows the current significant global NTL-RS data and the main parameters [18].

The NTL-RS data chosen for this study are the NPP Visible Infrared Imaging Radiometer Suite (NPP-VIIRS) 2020 annual average data. The spatial resolution of the NPP-VIIRS annual synthetic data is roughly 500 m. Solar radiation, lunar radiation, and transient light sources such as fire, aurora, and explosion [19] are removed from the annual average data processed by the system, and the noise value of the annual average data is minimized. The NPP-VIIRS data source is a global-scale image map. It must use ArcGIS software to cut the administrative area vector map of the target research area as a mask to produce the night light image map of the study area. The necessary georeferencing, projection conversion, and resampling through the nearest neighbor method are performed to obtain a nighttime light image with a standard 500 m spatial resolution. The preprocessed NTL-RS and SFS data were correlated using a graph model, and the GCRM and PCRM were determined by calculating the adjacency matrix.

Table 2. Simulation parameters of SFS data of digital TV

Digital TV	Geographic coordinates	Transmitting power (dBW)	Antenna height (m)	Feeder loss (dB)
Case A	25.054076, 102.703556	40	70	0

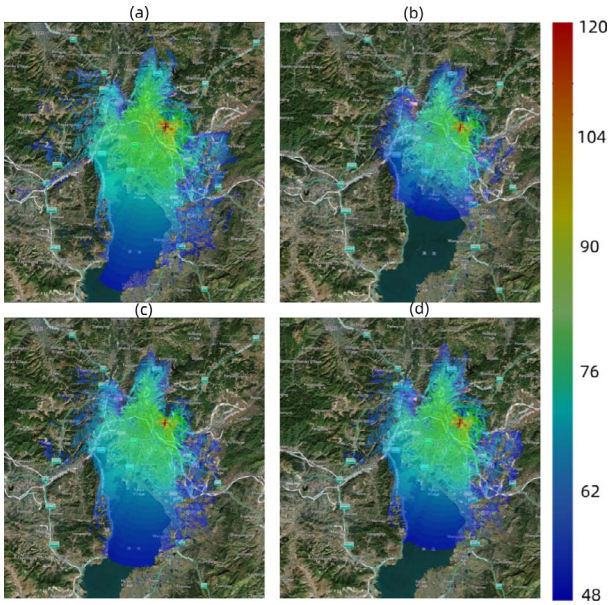

Figure 1. FM radio coverage map under different conditions.

4. Graph Model and Adjacency Matrix

The proposed radio monitoring coverage graph model based on NTL-RS and SFS data is represented by a three-layer structure:

$$G^t = (V^t, E^t, X^t) \tag{1}$$

Here, G^t denotes the graph model at time t, where t is the time when the NTL-RS data are selected, V^t is the node set, $N = |V|$ is the total number of nodes, including light nodes u and SFS nodes v, E is the edge set, $M = |E|$ is the total number of edges, X^t is used to denote the node attribute features, edge attribute features, and adjacency matrix A. The graph model denoted by (1) is shown in Figure 3. The SFS nodes v are divided into radio monitoring SFS nodes v_{I}^t, radio service nodes v_{II}^t, and frequency band nodes v_{III}^t, so there is a containment relationship between them, i.e., $v_{\mathrm{III}}^t \subset v_{\mathrm{II}}^t, v_{\mathrm{II}}^t \subset v_{\mathrm{I}}^t$. Accordingly, the light nodes u can be divided into nighttime light data u_{I}^t, nighttime light node

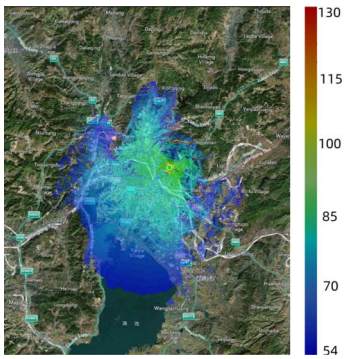

Figure 2. Digital TV coverage map.

Table 3. NTL-RS data and the main characteristic parameters[a]

Observation platform	Spatial resolution	Operational years
DMSP Operational Linescan System	2700 m	1992 to 2013
NPP-VIIRS	740 m	2013 to present
SAC-C HSC	200 m to 300 m	2001 to present
SAC-D HSC	200 m	2013 to present
International Space Station	30 m to 50 m	2000 to present
Loujia-101	130 m	2018 to 2019
VPAN-RS	<15 m	2021

[a] SAC: Scientific Applications Satellite; HSC: high sensitivity camera.

corresponding to radio service coverage u_{II}^{t}, and the nighttime light node corresponding to a certain radio frequency band u_{III}^{t}, $u_{\mathrm{III}}^{t} \subset u_{\mathrm{II}}^{t}, v_{\mathrm{II}}^{t} \subset u_{\mathrm{I}}^{t}$.

In radio broadcasting and communication applications, the SFS can only be perceived by users when it exceeds a certain threshold $E_{\min}$. Therefore, in addition to the same geographic location, the frequency band node v_{III} and the corresponding light node u_{III} must satisfy the requirement that the space field strength exceeds $E_{\min}$, and its value is determined by the node attribute characteristics and edge attribute characteristics. The adjacency matrix A_{vu} is expressed as

$$A_{vu} = \begin{pmatrix} e_{11} & \cdots & e_{1m} \\ \vdots & \ddots & \vdots \\ e_{n1} & \cdots & a_{nm} \end{pmatrix} \tag{2}$$

where $[1, 2, ...i..., n]$ and $[1, 2, ...j..., m]$ correspond to the geographic coordinates of the frequency band nodes v_{III} and the light nodes u_{III}, respectively. In the adjacency matrix A_{vu},$e_{ij} = 1, i = j, E \geq E_{\min}$ indicates that the geographic coordinates of the frequency band node $v_{\mathrm{III}i}$ and the light node $u_{\mathrm{III}j}$ are the same, and the SFS exceeds the threshold $E_{\min}$, so there is an adjacency between them. Also, $e_{ij} = 0, i = j, E < E_{\min}$ indicates that the geographic coordinates of the frequency band node $v_{\mathrm{III}i}$ and the light node $u_{\mathrm{III}j}$ are the same, but the SFS is less than the threshold $E_{\min}$, so there is no adjacency between them. Moreover, $e_{ij} = 0, i \neq j$ indicates that there is no adjacency between the frequency band nodes v_{III} and the light nodes u_{III} with different geographic coordinates.

Only the adjacency between lighting nodes and SFS nodes is considered in the definition of the adjacency matrix. The influence of node weights on the adjacency matrix is not taken into account. To more accurately characterize PCRM, this article defines the adjacency matrix with weights as follows:

$$A_{vu} = \begin{pmatrix} e_{11}w_{11} & \cdots & e_{1m}w_{1m} \\ \vdots & \ddots & \vdots \\ e_{n1}w_{n1} & \cdots & a_{nm}w_{nm} \end{pmatrix} \tag{3}$$

where w_{ij} is the weight of e_{ij}, characterized by the coupling coordination between the NTL u_i and the SFS node v_j, calculated using the coupling coordination model proposed in [20]. Assuming $\max(u_i, v_j) = u_i$, w_{ij} are calculated as follows:

$$w_{ij} = \sqrt{[1 - (u_i - v_j)] \times (v_j / u_i)} \tag{4}$$

Table 4. Assessment result of FM radio monitoring coverage

FM radio	NLC (%)	GCRM (%)	PCRM (%)	WPCRM (%)
Case A	58.8	27.96	57.5	94.3
Case B	58.8	17.91	44.6	91.9
Case C	58.8	22.90	49.8	93.1
Case D	58.8	23.00	51.0	93.3

NLC: Night Light Coverage

5. Definition and Calculation of Radio Monitoring Coverage

The radio monitoring coverage in this article is defined and calculated as follows. The nighttime light coverage is first computed as $R_l = N_l \div N_L$, where N_l is the number of lighting nodes with light value greater than 0 in the target study area and N_L is the total number of lighting nodes. The GCRM is then computed as $R_r = N_r \div N_R$, where N_r is the number of SFS nodes with value greater than or equal to 48 dBμv/m and N_R is the number of all SFS nodes. The PCRM is computed afterwards as $R_{\mathrm{p}} = N_{r+l} \div N_l$, where N_{r+l} is the number of light nodes with light value greater than 0 and SFS nodes with value greater than or equal to 48 dBμv/m with the same latitude and longitude. The weighted PCRM (WPCRM) is calculated as $R_{p_w} = V_l \div V_L$, where V_L is the total value of light nodes in the target study area and V_l is the total value of light nodes in the same geographic location of the SFS nodes with a value greater than or equal to 48 dB (millivolt per meter) for FM radio and 54.1 dB (millivolt per meter) for digital TV.

6. Results and Discussion

The target study area for this work is the Wuhua District in Kunming, Yunnan Province. The SFS data of FM radio and digital TV are simulated under various transmitting parameters and combined with NTL-RS data to evaluate the radio monitoring coverage. The statistical results are shown in Tables 4 and 5, and the values of the adjacency matrix are represented as points on the map shown in Figure 4, where Figures 4a–4d correspond to the simulation condition of Figures 1a–1d, respectively.

The previous results show that the FM radio's WPCRM in Wuhua District, Kunming, is 94.3% under the national standard simulation conditions. Reducing

Table 5. Assessment result of digital TV monitoring coverage

Digital TV	NLC (%)	GCRM (%)	PCRM (%)	WPCRM (%)
Case A	58.8	27.96	57.5	94.3

NLC: Night Light Coverage

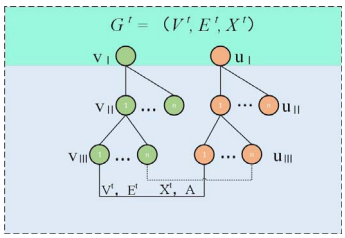

Figure 3. Graph model of wireless monitoring coverage.

transmit power, reducing antenna height, or increasing feeder loss decrease GCRM to varying degrees but have little impact on PCRM. According to Table 4, the GCRM of FM radio increases by 56.11% when the transmitting power goes from 1 kW to 10 kW, while the WPCRM only increases by 2.61%. When the height of the transmitting antenna is adjusted from 35 m to 70 m, GCRM increased by 22.01%, while WPCRM only increased by 1.29%. Also, when the path loss is reduced by 5 dB, GCRM of the FM radio increased by 21.57%, while WPCRM only increased by 1.07%. The same conclusion can be drawn for digital television. It is evident from the previously mentioned results that for plateau and mountainous areas, such as Yunnan Province, the performance of the monitoring station can be improved to increase GCRM of the radio monitoring station, but this has negligible impact on improving the PCRM.

7. Conclusion

The geographic coverage and population coverage of TV and FM radio in the Wuhua District of Kunming is studied based on the combination of NTL-RS data and SFS data. The results demonstrate that although enhancing the performance of radio monitoring stations for mountainous areas can significantly improve GCRM, it has little impact on PCRM. Therefore, the key to enhancing PCRM is to increase the number of spectrum sensing nodes or class IV radio monitoring stations. Compared with previous studies, the work presented in this article has the following advantages: 1) the combination of NTL-RS data and SFS data provides a new approach for the coverage capability assessment of radio monitoring stations from the perspective of population coverage; and 2) a graph model for complex data correlation is established, while the research methodology is universal and can be extended to other fields.

8. References

1. C. E. G. Moreta, M. R. C. Acosta, and I. Koo, "Prediction of Digital Terrestrial Television Coverage Using Machine Learning Regression," *IEEE Transactions on Broadcasting*, **65**, 4, March 2019, pp. 702-712.
2. D. Chen, M. Huang, and J. Yang, *Study of the Radio Spectrum Values*, Beijing, Science Publishers, 2021.
3. Ministry of Industry and Information Technology, *VHF/UHF Monitoring Network Function and Capability Assessment Specification*, report no. 016379-8, Ministry of Industry and Information Technology, Beijing, December 29, 2016.
4. M. Huang, J. Yang, M. Yang, and J. Chen, "VHF/UHF Fixed Monitoring Station Coverage Calculation and Preliminary Assessment," *Chinese Radio*, 2, February 2019, pp. 55-58.
5. Q. Lu, J. Yang, M. Huang, and Z. Jin, "Measurement and Evaluation of Radio Fixed Monitoring Station Coverage Capacity in China's Land Border Areas," *Chinese Radio*, **2**, February 2016, pp. 26-28.
6. Y. Zhang, M. Huang, and J. Yang, "Comparison of FM Radio Monitoring Coverage of VHF/UHF Fixed Monitoring Stations," *Chinese Radio*, **11**, November 2020, pp. 44-47.
7. P. Han, "Introduction to VHF/UHF Fixed Radio Monitoring Station Coverage Area Evaluation Scheme," *Chinese Radio*, **3**, March 2021, pp. 50-53.
8. C. E. Garcia Moreta, M. R. Camana Acosta, and I. Koo, "Prediction of Digital Terrestrial Television Coverage Using Machine Learning Regression," *IEEE Transactions on Broadcasting*, **65**, 4, December 2019, pp.702-712.
9. J. Zhang, X. Liu, and X. Tan, "Nighttime Vitality and Its Relationship to Urban Diversity: An Exploratory Analysis in Shenzhen, China," *IEEE Journal of Selected Topics in Applied Earth Observations and Remote Sensing*, **15**, 11, November 2021, pp. 309-322.
10. K. Shi, Y. Wu, and D. Li, "Population, GDP, and Carbon Emissions as Revealed by SNPP-VIIRS NTL-RS Data in China With Different Scales," *IEEE Geoscience and Remote Sensing Letters*, **19**, 8, August 2022, pp. 1-5.
11. Z. Chen, Y. Wei, K. Shi, Z. Zhao, C. Wang, et al., "The Potential of Nighttime Light Remote Sensing Data to Evaluate the Development of Digital Economy: A Case Study of China at the City Level," *Computers, Environment and Urban Systems*, **92**, 21, March 2022, p. 101749.
12. L. Gao, J. Liu, Y. Huang, and A. Men, "An Experimental Implementation of China Digital Radio (CDR) Broadcasting in Hubei," *IEEE Transactions on Broadcasting*, **68**, 3, September 2022, pp.797-801.

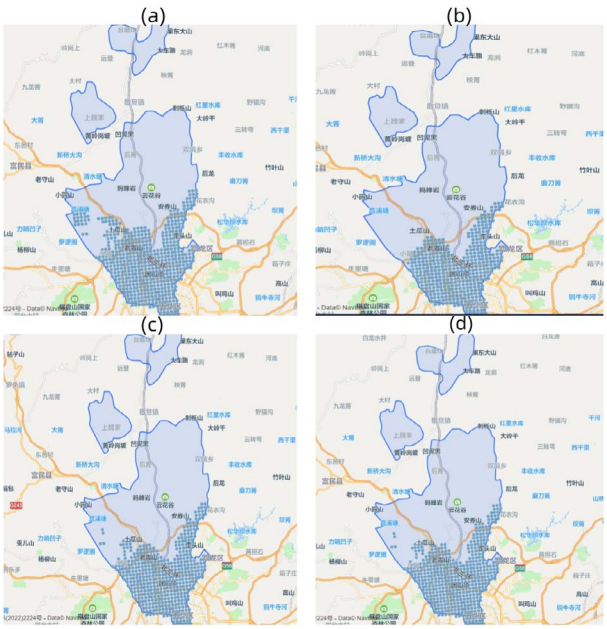

Figure 4. Adjacency matrix represented on the map under different conditions.

13. J. A. Kutzner and D. Lung, "Predicting ATSC 3.0 Broadcast Coverage," *IEEE Transactions on Broadcasting*, **62**, 1, March 2016, pp. 281-288.
14. O. Fratu, A. Martian, R. Craciunescu, A. Vulpe, S. Halunga, et al., "Comparative Study of Radio Mobile and ICS Telecom Propagation Prediction Models for DVB-T," IEEE International Symposium on Broadband Multimedia Systems and Broadcasting, Ghent, Belgium, June 17–19, 2015, pp. 1-6.
15. Q. Huang, X. Yang, and B. Gao, "Application of DMSP/OLS NTL Images: A Meta-Analysis and a Systematic Literature Review," *Remote Sensing*, **6**, 8, July 2014, pp. 6844-6866.
16. D. Hillger, T. Kopp, and T. Lee, "First-Light Imagery From Suomi NPP VIIRS," *Bulletin of the American Meteorological Society*, **94**, 7, July 2013, pp. 1019-1029.
17. C. Liu, Q. Tang, and Y. Xu, "High-Spatial-Resolution NTL Dataset Acquisition Based on Volunteered Passenger Aircraft Remote Sensing," *IEEE Transactions on Geoscience and Remote Sensing*, **60**, 12, December 2021, pp. 1-17.
18. N. Levin, C. C. M. Kyba, and Q. Zhang, "Remote Sensing of Night Lights: A Review and an Outlook for the Future," *Remote Sensing of Environment*, **237**, 2, February 2020, p. 111443.
19. Q. Zheng, Q. Weng, and K. Wang, "Developing a New Cross-Sensor Calibration Model for DMSP-OLS and Suomi-NPP VIIRS Light-Light Imageries," *ISPRS Journal of Photogrammetry and Remote Sensing*, **153**, 7, July 2019, pp. 36-47.
20. S. J. Wang, W. Kong, and L. Ren, "Misconceptions and Corrections of Coupled Coordination Degree Models in China," *Natural Resources Journal,* **36**, 3, March 2021, pp. 793-810.